Modeling and Estimation of Partially Observed WLAN Activity for Cognitive WSNs

Marcello Laganà, Ioannis Glaropoulos, Viktoria Fodor
Access Linnaeus Center
KTH, Royal Institute of Technology
10044, Stockholm, Sweden
Email: {lagana, ioannisg, vfodor}@kth.se

Chiara Petrioli
Dipartimento di Informatica
University of Rome "La Sapienza"
00198, Rome, Italy
Email: petrioli@di.uniroma1.it

Abstract—**Efficient communication in the crowded ISM band requires the communication networks to be aware of the networking environment and to control their communication protocols accordingly. In this paper we address the issue of efficient WSN communication under WLAN interference. We propose analytic models to describe the WLAN idle time distributions as observed by the WSN nodes, together with efficient methods for parameter estimation. We evaluate how the spectrum sensing capability of the sensors affects the performance of the idle period distribution estimation and conclude that the proposed solutions are accurate enough to support cognitive WSNs.**

I. INTRODUCTION

The spectrum of the open Industrial, Scientific and Medical (ISM) band is gradually becoming a scarce resource, due to the growing proliferation of wireless devices [1]. In this environment the network protocols, often optimized for the standalone network, do not anymore provide the required communication efficiency or performance guarantees. In this paper we focus on the challenge of efficient WSN communication when a WLAN operates in the same area. As WLAN carrier sensing is designed to detect WLAN signals, it is *blind* towards the low power, narrow band WSN transmissions. As a consequence, the WLAN causes harmful interference in the WSN, while itself remains unaffected from the WSN interferers. The WSN nodes can avoid WLAN interference and thus costly packet retransmissions only if they are armed with cognitive capabilities [2], i.e they are aware of the WLAN behavior and optimize their transmission parameters and communication protocols accordingly.

Previous work in the area of cognitive WSNs includes proposals for novel carrier sensing and medium access control, and the characterization of the channel usage in WLAN cells. In [3] the interfering technology is identified based on spectral signature. In the case of WLAN interferers, the sensors force the WLAN to back off by sending short, high power jamming signals. The POMDP framework [4] introduces the concept of partial channel knowledge and proposes optimal sensing and channel access strategies considering a Markovian channel occupancy model. A Markovian model, however, may lead to suboptimal WSN operation, and therefore several works deal with a more accurate channel characterization. In [5] the WLAN output buffers are modeled as M/G/1 queues, resulting in sub-geometric idle period distribution. In [6] an hyper-exponential distribution is fitted to the empirical idle period distribution derived by traffic traces from an area with heterogeneous wireless devices. In [7] the idle periods are modeled with a Pareto distribution, and packet lengths are optimized accordingly to control the collision probability. In our work we follow the model of [8][9], where a mixture distribution is proposed to model the idle periods, capturing the two basic sources of inactivity, the short, almost uniformly distributed contention windows and the long, heavy-tailed white space periods, when the WLAN users are inactive.

Our goal is to evaluate whether the sensor nodes are capable of estimating the channel occupancy model parameters by performing continuous sensing for limited time intervals. We enhance the model of [8] with a *Local View* component to take the limited detection range of the sensor nodes into account, and propose computationally efficient ways to estimate the model parameters from idle and active period measurements, using likelihood maximization and neural networks based learning algorithms.

The rest of the paper is organized as follows. Section II defines the considered networking scenario along with the WLAN channel activity models. In Section III we propose estimation algorithms based on Laplace Transforms and Neural Networks, while in Sections IV and V we evaluate their accuracy based on numerical and simulation results. We conclude the paper in Section VI.

II. SYSTEM MODEL

A. Networking Scenario

We consider an IEEE 802.15.4 compliant WSN operating in the transmission area of a IEEE 802.11 WLAN. The transmission power of the WLAN terminals is orders of magnitude higher than that of the coexisting WSN, and the WLAN terminals are *blind* towards the WSN transmissions. The protocol stack of the energy constrained WSN is enhanced by cognitive functionality to optimize the WSN operation. The cognitive control consists of two phases.

First, the sensors perform continuous sensing, and collect samples of busy and idle WLAN period lengths. Based on the collected data, they estimate the parameters of the WLAN channel occupancy distributions. The sensing is based on the usual Clear Channel Assessment (CCA) process with energy
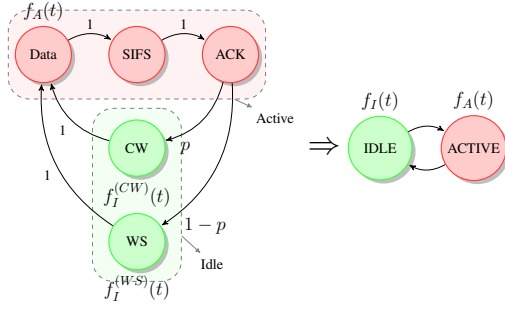
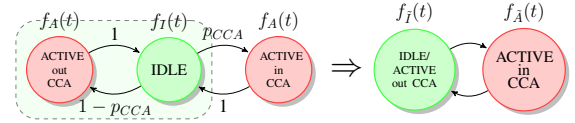Fig. 1: The Global View model with all channel states and the reduced two-state semi-Markovian model.

Fig. 2: The 3-state semi-Markovian chain and its 2-state equivalent for the Local View channel activity modeling.

detection, resulting in a limited sensing range. The sensing and estimation process is repeated with low frequency to follow the traffic intensity changes in the WLAN [10].

Second, based on the results of the estimation process the sensors optimize their transmission parameters to fulfill some performance requirement, for example, control the probability of packet loss due to WLAN interference [7], or minimize energy consumption [11].

This paper deals with the first phase and evaluates the achievable parameter estimation accuracy and the related sensing cost, leaving the transmission optimization for future work.

B. WLAN spectrum occupancy modeling

We consider the semi-Markovian system of active and idle periods to model the stochastic WLAN channel occupancy, as proposed in [8]. We call this model as the *Global View*, since it takes all WLAN activity into account. Figure 1 depicts all the states of the WLAN channel and their merging into a two-state semi-Markovian chain. The states of Data, SIFS and ACK transmission are grouped together into a single *Active* state, and the states that represent the WLAN Contention Window period (CW) and the WLAN White Space (WS) due to user inactivity are merged into a single *Idle* state.

To predict how long the system remains in either state, we need to derive the distributions $f_A(t)$ and $f_I(t)$ for the sojourn times in the Active and Idle state, respectively. As shown in [8], the *uniform* distribution sufficiently models the active and the CW periods, with ranges $[\alpha_{\mathrm{ON}}, \beta_{\mathrm{ON}}]$ and $[0, \alpha_{\mathrm{BK}}]$, $\alpha_{\mathrm{BK}} \le \alpha_{\mathrm{ON}}$, respectively. The WS periods, however, exhibit a heavy-tailed behavior that is well approximated by a zero-location *generalized Pareto* distribution with parameters (ξ, σ). The idle period distribution, $f_I(t)$, is therefore represented by a *mixture* distribution with a weight p [9]: $f_I(t) \triangleq p \cdot f_I^{CW}(t) + (1-p) \cdot f_I^{WS}(t)$, where the $f_I^{CW}(t)$ is the uniform distribution in the back-off range and $f_I^{WS}(t)$ is a generalized Pareto distribution of the white spaces and consequently $f_I(t)$ is:

$$f_I(t) \triangleq \begin{cases} p \cdot \dfrac{1}{\alpha_{\mathrm{BK}}} + (1-p) \cdot \dfrac{1}{\sigma}\left(1+\xi\dfrac{t}{\sigma}\right)^{\left(-\frac{1}{\xi}-1\right)} & t \le \alpha_{\mathrm{BK}} \\ (1-p)\dfrac{1}{\sigma}\left(1+\xi\dfrac{t}{\sigma}\right)^{\left(-\frac{1}{\xi}-1\right)} & t > \alpha_{\mathrm{BK}} \end{cases}$$

We extend the above Global View model and define the *Local View*, that describes the WLAN channel occupancy as seen by an individual sensor with limited sensing range. Assuming that consecutive WLAN transmissions are not correlated, we introduce a 3-state semi-Markovian system (Figure 2), distinguishing between detected, and un-detected WLAN activity, that occurs with probability p_{CCA} and $(1-p_{\mathrm{CCA}})$, respectively. To model the *observable* sojourn time distributions $f_{\tilde{A}}(t)$ and $f_{\tilde{I}}(t)$ we define the 2-state *Local View* model by merging the states at which the sensor detects an idle channel. It holds that $f_{\tilde{A}}(t) = f_A(t)$, but $f_{\tilde{I}}(t) \ne f_I(t)$, $\forall p_{\mathrm{CCA}} < 1$.

Our objective is to estimate the parameters of $f_A(t)$ and $f_I(t)$ and the *observable load*, p_{CCA}, from a set of samples of $f_{\tilde{A}}(t)$ and $f_{\tilde{I}}(t)$ obtained through channel sensing.

III. LOCAL VIEW PARAMETER ESTIMATION

As the active period distribution, $f_{\tilde{A}}(t)$, is uniform, its parameters α_{ON} and β_{ON} are estimated by the lowest and the largest measured active period according to Maximum Likelihood Estimation (MLE). For the rest of the paper we assume that the active distribution is estimated perfectly. The parameter estimation of the Global View idle period, $f_I(t)$, is addressed in [8]. Assuming that the maximum back-off time, α_{BK}, is given by the WLAN specification, the Pareto parameters ξ and σ can be derived with MLE, by discarding all observations in the range of $[0, \alpha_{\mathrm{BK}}]$[12], while the weight p can be derived through Moment Evaluation (ME).

Let us consider the Local View model. An idle channel period observed by an arbitrary sensor consists of a random number of WLAN "cycles", that is, consecutive idle and un-detected active periods, followed by an additional idle period. The locally observable idle period distribution, $f_{\tilde{I}}(t)$, is, therefore, a function of the idle and active time distributions $f_I(t)$ and $f_A(t)$, and of the observable load, p_{CCA}, and can not be expressed in a closed form, even if $f_A(t)$ is known. The lack of a closed form expression prevents us from applying MLE directly on the sample series of observed idle periods, and an alternative solution is needed for the parameter estimation.

A. Parameter Estimation in the Laplace Domain

Contrary to the density function, the Laplace Transform (LT) of the locally observed idle period distribution, $f_{\tilde{I}}^*(s)$, can be derived in a closed-form, as follows. The LT of the WLAN cycle is $f_{\mathcal{C}}^*(s) = f_I^*(s)f_A^*(s)$, where $f_A^*(s)$ is the LT of the uniformly distributed active periods and $f_I^*(s)$ is the LT of the linear combination of the uniformly distributed CW and the Pareto distributed WS periods. As in the Local

View model the number of consecutive cycles has geometric distribution with parameter p_{CCA}, the LT of the sum of the WLAN cycles is $f_{\tilde{C}}^*(s) = \mathcal{P}_K\{f_C^*(s)\}$, with Zeta transform $\mathcal{P}_K(z) = p_{CCA}/(1 - (1 - p_{CCA})z)$. Since the observable idle period includes an additional idle time before a detected WLAN activity period, we finally have:

$$f_I^*(s) = f_I^*(s)\frac{p_{CCA}}{1 - (1 - p_{CCA})f_I^*(s)f_A^*(s)}. \quad (1)$$

We derive the empirical LT of the observable idle time distribution, $f_{\tilde{I}e}^*(s)$ directly from the N measured idle period samples, $(t_1,...,t_N)$:

$$f_{\tilde{I}e}^*(s; N) = \frac{1}{N}\sum_{i=1}^{N} e^{-st_i}. \quad (2)$$

To estimate the Local View model parameters we aim at minimizing the Mean Square Error (MSE) between the empirical and the analytic LT in (1), evaluated on a finite discrete subset of the s-domain, $\mathcal{S} = \{s_1, s_2,...s_S\}$:

$$(\hat{\xi}, \hat{\sigma}, \hat{p}, \hat{p}_{CCA}) =$$
$$\arg\min \frac{1}{S}\sum_{k=1}^{S}(f_{\tilde{I}e}^*(s_k; N) - f_{\tilde{I}}^*(s_k; \xi, \sigma, p, p_{CCA}))^2. \quad (3)$$

In addition to applying exhaustive search, we derive $(\hat{\xi}, \hat{\sigma}, \hat{p}, \hat{p}_{CCA})$ in (3) by adapting the discrete space global iterative search method proposed in [13]. The 4-dimensional search space is reduced by using ME to express p_{CCA} from the rest of the parameters. The iterative process runs parallel to the channel sensing. In each iteration n_m new idle period samples are integrated, and $f_{\tilde{I}e}^*(s; N)$ is recalculated according to (2). We define the discrete search space, $\mathcal{K} = \{\mathcal{K}_1,...,\mathcal{K}_K\}$, where $\{\xi_i, \sigma_i, p_i\}$ is the set of parameters for the state $\mathcal{K}_i$. The search process moves from state to state randomly, until a stopping condition is triggered, as given by Algorithm 1. The algorithm stops, if its state has been unchanged for π_{max} iterations, or when the sensing is completed and all the N samples are integrated. $\{\hat{\xi}, \hat{\sigma}, \hat{p}\}$ is then given by the most visited state, denoted as $\mathcal{K}^*$. We denote by $Q_m(\mathcal{K}_j)$ the number of times state $\mathcal{K}_j$ has been visited until the m-th iteration, and by π_m the number of successive iterations the algorithm state remained unchanged after iteration m.

Algorithm 1. *Initialization: Select a starting state* $\mathcal{K}_0 = (\xi_0, \sigma_0, p_0) \in \mathcal{K}$ *randomly. Let* $\pi_0 = 1$, $Q_0(\mathcal{K}_0) = 1$, $Q_0(\mathcal{K}_j) = 0, \forall\mathcal{K}_j \in \mathcal{K}$.
Iteration $m \geq 1$: *Choose a state* $\mathcal{J}_m = \{\xi_m, \sigma_m, p_m\} \in \mathcal{K}\backslash\{\mathcal{K}_{m-1}\}$ *with probability* $\frac{1}{K-1}$.
Integrate n_m *new samples of the idle series.*
Let $f_{\tilde{I}e}^*(s; N_m) = 1/N_m\sum_k e^{-st_k}, s \in \mathcal{S}$, $N_m = \sum_{l=1}^{m} n_l$.
Let $MSE_m = \frac{1}{S}\sum_{k=1}^{S}(f_{\tilde{I}e}^*(s_k; N_m) - f_{\tilde{I}}^*(s_k; \mathcal{J}_m))^2$.
If $MSE_m < MSE_{m-1}$, $\mathcal{K}_m = \mathcal{J}_m$ *and* $\pi_m = 1$, *otherwise* $\mathcal{K}_m = \mathcal{K}_{m-1}$ *and* $\pi_m = \pi_{m-1} + 1$. *Let* $Q_m(\mathcal{K}_m) = Q_{m-1}(\mathcal{K}_m) + 1$. *If* $\pi_m \geq \pi_{max}$ *or* $N_m = N$, **Stop.**
Output: *Let* $\mathcal{K}^* = \arg\max_{\mathcal{K}_j \in \mathcal{K}} Q_m(\mathcal{K}_j)$.

The computational complexity of each step is linear with $|\mathcal{S}|$, while the required memory is proportional to the size of $\mathcal{K}$. The algorithm converges almost always to the optimum state, as we show in [14]. We have to note, however, that MSE minimization in the Laplace domain does not necessarily lead to likelihood maximization in the time domain, which may decrease the accuracy of the parameter estimation.

B. Parameter Estimation with Neural Network

The Neural Network (NN) is a computational paradigm for artificial intelligence, modeled after the human brain and nervous system. We implement an NN to estimate the parameters of $f_{\tilde{I}}(t)$ in time domain, without knowing its closed form.

An NN consists of a set of connected neurons organized in layers, where each neuron forwards to the next layer the linear combination of the values received from the previous layer or layers. The first – input – layer receives values from outside the network, the last – output – layer returns values of the output parameters of interest, and the layers in between remain hidden [15]. To use the NN for parameter estimation, we first train it with a set of training vectors with known input and output values, setting the weights of the connections between the neurons. Once the training phase is completed, the parameterized NN can be deployed on the sensors using a very limited memory and can derive the outputs for new input vectors in linear time.

We consider an NN with a single hidden layer (Figure 3), where the number of hidden neurons is half of the number of the input ones. The output layer consists of the four-ordered vector of estimated parameters, $(\hat{\xi}, \hat{\sigma}, \hat{p}, \hat{p}_{CCA})$. When defining the input layer our goal is to introduce a structure that is decoupled from the number of measured idle time samples. Therefore we build the empirical PDF of the N measured idle period samples, $(t_1,...,t_N)$, and choose a set of $\mathcal{X} = \{x_1,...,x_X\}$ points as the input of the NN. We sample the empirical PDF according to a logarithmic scale so as to capture the distinctive part of the Pareto WS distribution. To increase estimation accuracy, the input layer receives also the idle time sample mean (μ) and variance (σ^2), as well as the $f_A(t)$ parameters obtained via MLE. The CW parameter α_{BK} is assumed to be known as mentioned earlier. The training is performed with the RPROP algorithm proposed in [16].
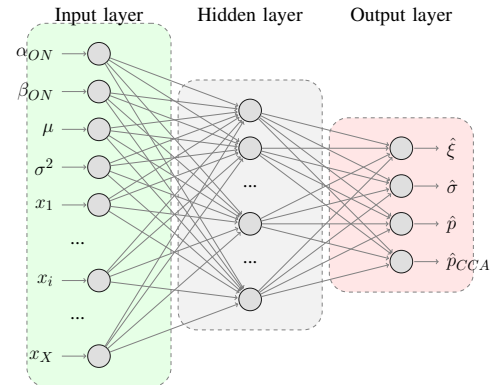

Fig. 3: Neural Network for parameter estimation.

IV. NUMERICAL PERFORMANCE EVALUATION

In this section we evaluate the accuracy of the proposed LT and NN based estimation. We select 10^4 $(\xi, \sigma, p, p_{CCA})$ param-
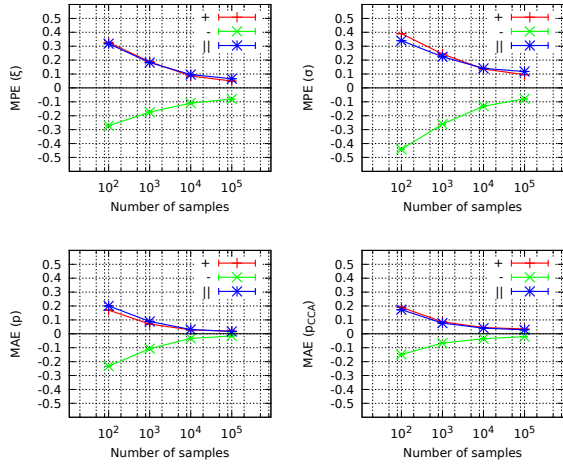
Fig. 4: The accuracy of the LT-based estimation with respect to the number of idle period samples. Results with index $+$ and $-$ show averages for over and under estimations.

Fig. 5: The accuracy of the LT-based estimation algorithm with respect to the observable load, p_{CCA}. $N = 10^4$ samples.

eter vectors, generate a sequence of idle and active periods for each vector, and run the estimation algorithms. The parameters are randomized according to Table I, to cover a wide range of traffic patterns. As stated in Section III it is assumed that the $f_A(t)$ parameters can be estimated correctly and α_{BK} is known. We measure the sensing accuracy by calculating the mean absolute error (MAE) of the p and p_{CCA} and the mean percentage error (MPE) of the ξ and σ estimation. We evaluate, how the estimation accuracy changes with N, the number of collected observable idle period samples, since this quantity reflects the required sensing time.

TABLE I: Model Parameters

Parameter	Distribution	Min	Max	Mean	StdDev
ξ	Truncated Gaussian	0.1	0.4	0.3095	0.1
σ	Truncated Gaussian	1e-4	0.1	0.02	0.2
p	Uniform	0.1	1.0		
p_{CCA}	Uniform	0.1	1.0		
α_{ON}	Uniform	0.0008	0.001		
β_{ON}	Uniform	α_{ON}	0.0015		
α_{BK}	Deterministic			0.0007	

A. LT-based Parameter Estimation

The performance of the LT based parameter estimation depends not only on the traffic parameters, but also on S, the considered number of s-domain points, and the parameters of the discrete stochastic optimization. For the evaluations presented here we fix $S = 10^3$, $s_k \in (10^0, 10^5), 1 \le k \le S$, $n_m = 1, \pi_{\max} = N/2$, and select $\{\xi_i, \sigma_i, p_i\}$ with granularity 10^{-4} to define the states $\mathcal{K}_i = \{\xi_i, \sigma_i, p_i\}$, unless otherwise stated. We additionally implement an exhaustive search algorithm with a granularity of 10^4 for performance comparison.

Figure 4 depicts the accuracy of the iterative LT-based estimation algorithm with respect to N, the total number of idle period samples gathered in the sensing time. We consider
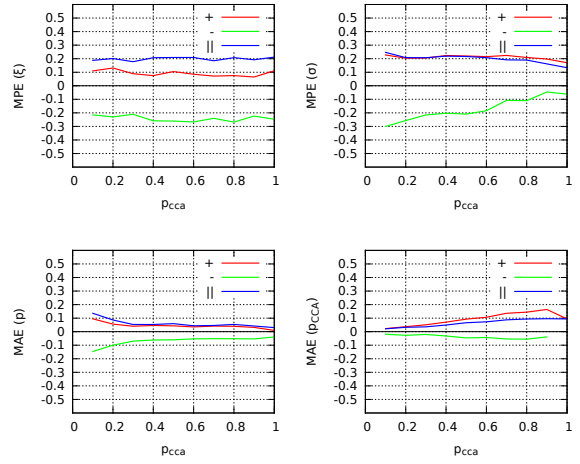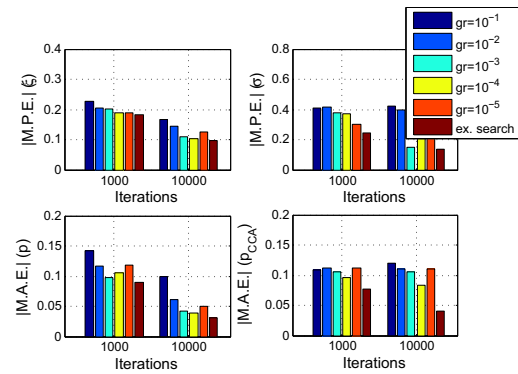

Fig. 6: The accuracy of the LT-based estimation with respect to the number of iterations, and the granularity of the state space. Exhaustive search results are shown for comparison.

MAE and MPE values averaged over all results, and averaged over results with over and under estimation. The estimation accuracy is, clearly, an increasing function of the number of considered samples. The LT-based estimation is very accurate for the model coefficients, p an p_{CCA} while it shows a higher – but still acceptable – error for the Pareto parameters. An observed idle period sample size of 10^4 results in excellent accuracy. For low observable WLAN load cases, however, a sample size of 10^3 still gives sufficient accuracy while keeping the sensing time in the order of seconds.

Since the distribution of $f_{\bar{I}}(t)$ depends significantly on the observable load parameter, p_{CCA}, we investigate how its value affects the estimation accuracy. As shown in Figure 5, the estimation quality increases only marginally with p_{CCA}, apart from the p_{CCA} values themselves, where the increasing MAE reflects a constant percentage error. Therefore, we can conclude that the LT-based algorithm can achieve a good approximation of the Global View parameters, ξ, σ and p from the locally observed time series, even in the case of small p_{CCA}.

Finally, Figure 6 evaluates the effect of the size of the state space of the discrete optimization. We change the granularity of the state parameters $\{\xi_i, \sigma_i, p_i\}$ from 10^{-1} to 10^{-5} to increase the state space. The results show that the performance of the proposed algorithm is comparable to the one of the exhaustive search. The accuracy increases with increased state space for a while, but after a point the state space becomes too large and the minimizer can not be discovered in the limited number of iterations. Therefore the granularity needs to be optimized according to the sample size N.

B. NN-based Parameter Estimation

To evaluate the performance of the NN-based parameter estimation we keep the NN structure fixed and consider 200 sample points from the empirical idle time distribution as NN inputs. We train the network with 10^4 training sequences, with input vectors selected according to Table I.
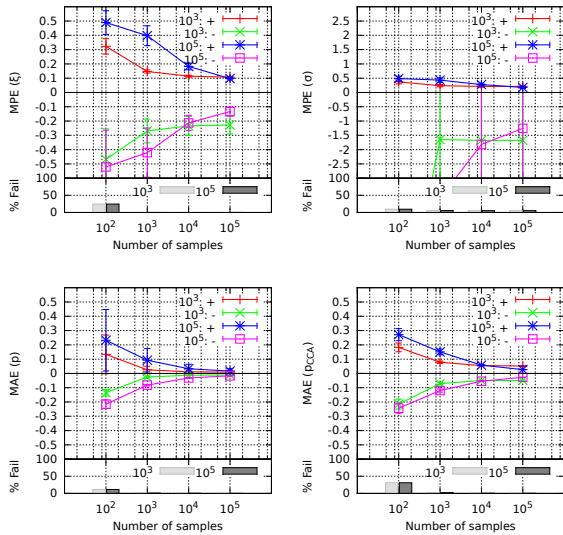

Fig. 7: The accuracy of the NN-based estimation with respect to the number of the idle period samples. Results with index $+$ and $-$ show averages for over and under estimations. Training vectors from 10^3 and 10^5 idle period samples are considered.

Figure 7 depicts the accuracy of the NN-based parameter estimation with respect to the number of idle period samples, N, considering training vectors from 10^3 and 10^5 idle period samples. It also shows the percentage of *Missed Estimation* (Fail) events, when an output neutron retrieves a value out of the parameter's range, for instance, $\hat{\sigma} < 0$ or $\hat{p} \notin [0, 1]$ etc. We notice the counter-intuitive result, that the training dataset from larger idle samples' size results in lower sensing accuracy. This happens because the neural network learned how to estimate parameters from examples finer than the tested ones and it expects data with the same, or even better precision. The achieved accuracy shows the same trends as in the case of the LT-based estimation, with marginally improved values for p, p_{CCA} and worse for ξ, σ. Notice, that the high MPE^-

TABLE II: WLAN Configuration Parameters

WLAN range	100m	Tx-Rate (ρ_{WLAN})	11Mbps
Number of Users	5	Path-Loss Exp. (α)	2.5
WU Tx-Power (P_{WU})	15dBm	Ref. Distance (d_0)	1m
AP Tx-Power (P_{AP})	15dBm	Noise Power (σ_N^2)	-174 dB/Hz

values for σ come from rare cases of parameter overestimation, and do not affect the average performance significantly.

Comparing the LT and the NN solutions we can see that the NN achieves slightly worse accuracy and at the same time misses the estimation with low probability. The algorithmic complexity is, however, different in the two cases. The LT-based estimation requires relatively complex calculations for the parameter estimation, while only the off-line training is complex in the Neural Network method.

V. EVALUATION OF ESTIMATION ACCURACY IN A WSN – SIMULATION STUDY

While the previous results give us valuable insight on the average estimation accuracy they do not show whether sensors in a WSN will have a similar understanding of the channel occupancy distribution, a desirable property for efficient cognitive networking. Therefore, we perform simulation-based evaluation, using the NS-Miracle framework [17] and implementing the NN-based parameter estimation.

We consider a single IEEE 802.11b WLAN Access Point (AP) and 5 Wireless Users (WUs) placed arbitrarily inside the coverage area around the AP. The WUs are stationary and operate in a "high SNR regime", thus the collision probability in the WLAN is negligible. We inject traffic in the WLAN by generating active and idle periods according to the Global View model and parameters from Table I. We randomly assign each active period with equal probability to the AP or any of the WUs, which transmit a packet with the corresponding frame-in-the-air duration. For the WSN we consider a fixed network on a square grid, where the distance between adjacent sensors is 30m. For each sensor we implement the IEEE 802.15.4 CCA process, and deploy an NN trained with input vectors from Table I. We consider a simple, path-loss propagation model for the WLAN-WSN link and set the WSN sensitivity so that each sensor has a disc shaped CCA area with 35m radius. The presented results are based on 10^4 simulation runs with fixed WU locations but randomized Global View parameter values. Table II summarizes the configuration of the networking environment.

We restrict the analysis to the WSN nodes that have at least one WLAN transmitter in their CCA area, which gives us the topology depicted in Figure 8. We aim at comparing the estimation results of all these sensors and also the estimation accuracy of the sensors that have the same p_{CCA} values, but observe different WLAN devices, therefore these are distinguished in the Figure.

Figure 9 shows, as an example, the average estimation error of the weight p, for 10^4 samples, at the sensors with $p_{CCA} > 0$. The achieved accuracy is quite similar across the sensors and
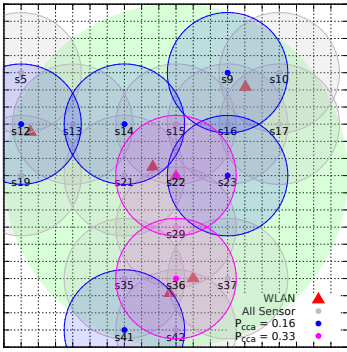
Fig. 8: The WLAN and the WSN topologies in the simulator.

slightly lower than the one in the numerical evaluation in Figure 7, probably because the experienced p_{CCA} values are now fixed. In Figure 10 we evaluate – by averaging over 10^4 simulation runs – the estimation error variations among the sensors within each run. We calculate the Coefficient of Variation (CV) of the error (MAE or MPE) across the sensors and depict its mean and standard deviation value. The resulting small value of the CV shows that the sensors achieve a consensus for all the estimated parameters, with slightly larger variations when considering sensors with different observable load parameter, p_{CCA}. From these results we can conclude that the traffic parameter values estimated by the individual sensors are sufficiently close to each other, and sensors estimate a similar Global View, despite their limited sensing capabilities.
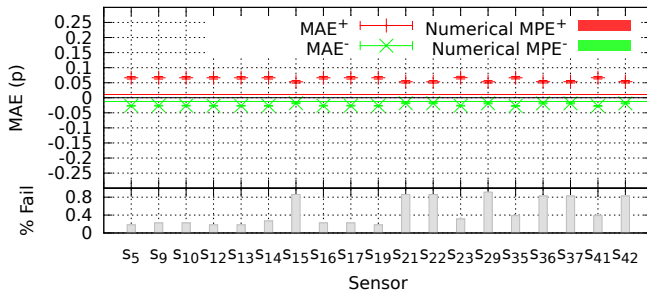

Fig. 9: Average p-estimation error on each sensor with $p_{CCA} > 0$, based on simulation. The solid lines correspond to the numerically evaluated error according to the NN algorithm.
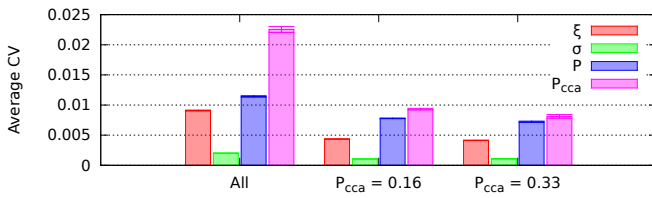

Fig. 10: Coefficient of Variation of the estimation errors at the sensors that are grouped according to the experienced p_{CCA} over 10^4 simulation runs. $N = 10^4$ samples.

VI. CONCLUSIONS

In this work we evaluated the capability of limited detection range WSN nodes to parameterize a WLAN channel occupancy model based on local sensing. We considered MSE minimization in the Laplace domain and NN based parameter estimation, and concluded, that both of them provide accurate results, while the LT-based solution shows higher reliability and the NN solution has slightly worse accuracy but significantly lower computational complexity. Therefore, when selecting the preferable solution the requirements towards reliability and the available computational resources at the sensors have to be considered.

REFERENCES

[1] I. F. Akyildiz, W. Lee, and K. R. Chowdhury. CRAHNs: Cognitive radio ad hoc networks. *Ad Hoc Networks*, 7(5):810 – 836, January 2009.

[2] S. Haykin. Cognitive radio: brain-empowered wireless communications. *IEEE Journal on Selected Areas in Communications*, 23(2):201 – 220, February 2005.

[3] K.R. Chowdhury and I.F. Akyildiz. Interferer classification, channel selection and transmission adaptation for wireless sensor networks. In *Proceedings of IEEE ICC'09*, pages 1 –5, June 2009.

[4] Q. Zhao, L. Tong, A. Swami, and Y. Chen. Decentralized cognitive MAC for opportunistic spectrum access in ad hoc networks: A POMDP framework. *IEEE Journal on Selected Areas in Communications*, 25(3):589 –600, April 2007.

[5] J. Misic and V.B. Misic. Characterization of idle periods in IEEE 802.11e networks. In *Proceedings of IEEE Wireless Communications and Networking Conference (WCNC)*, pages 1004 –1009, March 2011.

[6] L. Stabellini. Quantifying and modeling spectrum opportunities in a real wireless environment. In *Proceedings of Wireless Communications and Networking Conference (WCNC)*, pages 1 –6, April 2010.

[7] J. Huang, G. Xing, G Zhou, and R. Zhou. Beyond co-existence: Exploiting WiFi white space for Zigbee performance assurance. In *Proceedings of 18th IEEE International Conference on Network Protocols*, ICNP 2010, pages 305–314, October 2010.

[8] S. Geirhofer, L. Tong, and B.M. Sadler. Cognitive medium access: Constraining interference based on experimental models. *IEEE Journal on Selected Areas in Communications*, 26(1):95–105, January 2008.

[9] S. Geirhofer, J. Z. Sun, L. Tong, and B. M. Sadler. Cognitive frequency hopping based on interference prediction: theory and experimental results. *ACM SIGMOBILE Mob. Comput. Commun. Rev.*, 13:49–61, September 2009.

[10] H. F. Campos, M. Karaliopoulos, M. Papadopouli, and H. Shen. Spatio-temporal modeling of traffic workload in a campus WLAN. In *Proceedings of ACM SIGMOBILE 2nd Annual International Wireless Internet Conference (WICON)*, August 2006.

[11] I. Glaropoulos, V. Fodor, L. Pescosolido, and C. Petrioli. Cognitive WSN transmission control for energy efficiency under WLAN coexistence. In *Proceedings of ICST 6th Cognitive Radio Oriented Wireless Networks and Communications*, June 2011.

[12] J. d. Castillo and J. Daoudi. Estimation of the generalized pareto distribution. *Statistics & Probability Letters*, 79(5):684 – 688, 2009.

[13] S. Andradottir. A global search method for discrete stochastic optimization. *SIAM Journal on Optimization*, 6(2):513–530, 1996.

[14] I. Glaropoulos. Parameter estimation of partially observed WLAN spectrum activity via discrete stochastic optimization. Technical report, Royal Institute of Technology (KTH), September 2011.

[15] M. H. Hassoun. *Fundamentals of Artificial Neural Networks*. MIT Press, Cambridge, MA, USA, 1st edition, 1995.

[16] M. Riedmiller and H. Braun. A direct adaptive method for faster backpropagation learning: the RPROP algorithm. In *Proceedings of IEEE International Conference on Neural Networks (ICNN)*, pages 586 –591 vol.1, March 1993.

[17] *NS-Miracle: Multi-InteRfAce Cross-Layer Extension library for the Network Simulator*. http://telecom.dei.unipd.it/pages/read/58/.